Low energy ion scattering and scanning tunneling microscopy for surface structure analysis

S. Speller and W. Heiland

FB Physik, Universität Osnabrück, D-49069 Osnabrück, Germany

Abstract. Low energy ion scattering (ISS) and scanning tunneling microscopy (STM) are powerful tools for the analysis of surface structures. Both techniques are operative in real space. The ion scattering techniques afford quantitative data on surface structure but as spatial averages only. STM provides non-averaged local information but it is not necessarily quantitative. STM provides detailed information on surface defects, e. g. steps, and mesoscopic structures. The two techniques will be compared in the case of (110) surfaces of Au and Pb.

INTRODUCTION

Surface structure analysis has reached a new aera since the invention of the scanning tunneling microscope [1]. This new tool was preceeded by approximately 20 years of surface analysis using a large number of different techniques based on different basic phenomena of physics. Au(110) was the first surface found to exhibit reconstruction [2]. Reconstruction means, that actual surface is in a regular way different from the crystallographic structure of an equivalent plane in the bulk of the material. If the surface plane is equal in structure to the equivalent planes in the bulk, the situation is called "bulk terminated". Additionally to reconstruction there is a change of lattice parameters such that the planar distance between the outermost layer and the second layer, is changed. In most materials the change is a reduction called "contraction". The "standard data" for Au(110) are: the surface is (1x2) reconstructed with a contraction of 0.29Å and a lateral shift in the [001] direction of the [110] rows in the 2nd layer by 0.14Å [3]. Fig. 1 shows a model of a regular (1x1) surface of a fcc metal and a (1x2) reconstructed surface. For obvious reasons this structure is called "missing row" structure. Beside on Au (110) this type of reconstruction is also found on Pt(110).

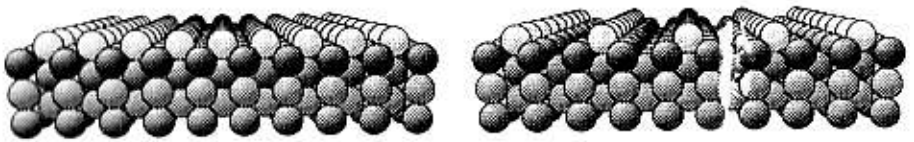

FIGURE 1: Model (perspective view) of a regular fcc (110) surface and of (1x2) reconstructed surface. The reconstructed phase has been named "missing row" structure.

STRUCTURE OF THE AU(110) SURFACE: ISS-RESULTS

The data presented have been published in the past in a number of papers. With respect to structural data good agreement was obtained with the LEED data [3, 4, 5]. Fig. 2 [6, 7] shows experimental ISS spectra in comparison with calculated spectra using the code MARLOWE. The code includes a simulation of the thermal displacement of the surface atoms. The "philosophy" is equivalent to the LEED analysis, i. e. a surface structure model is used based on the so called R-factor analysis. Best agreement is reached with the Moritz and Wolf model [4, 5]. The "saw tooth" model [8] e. g. is by all means not satisfactory (Fig. 2). For further details see the original papers [6, 7].

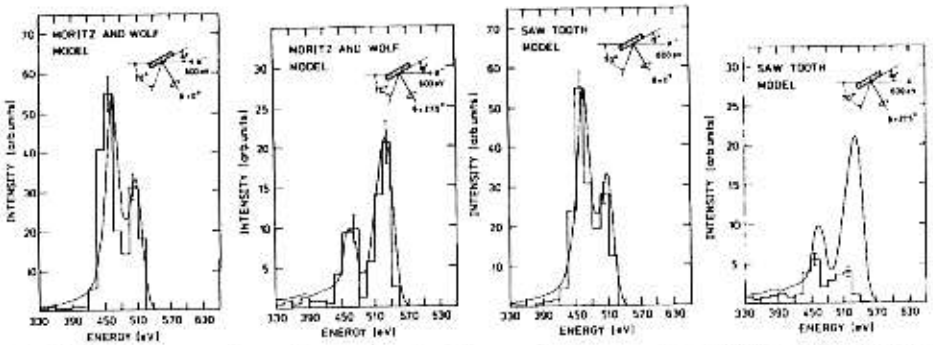

FIGURE 2: Comparison of experimental ion scattering spectra of K^+ scattered from Au(110)(1x2) [6] in comparison with calculated spectra (histograms)[7]. The calculated spectra are obtained from the structural models of Moritz and Wolf [4, 5] and the saw tooth model [8] respectively.

It is worth mentioning that the LEED analysis [4, 5, 9] included not only the "standard structural" data but also a detailed analysis of possible "defects" on fcc (110) surfaces, which includes (1x1), (1x2), (1x3), ... islands bordered by the necessary steps which connect the different areas. In short, the LEED analysis led to a real space surface which is dominated by the (1x2) reconstruction, but is organised in a mesa-like pattern with average dimensions of about 60Å along the $[1\bar{1}0]$ direction and of about 30Å along [001]. It would have been interesting to have had an "in situ" STM analysis of the same surface,

because recent STM results show much larger terraces in average [10, 11, 12] and obvioulsy, there are no extended [001] steps. The surface forms the so called "fish" scale pattern.

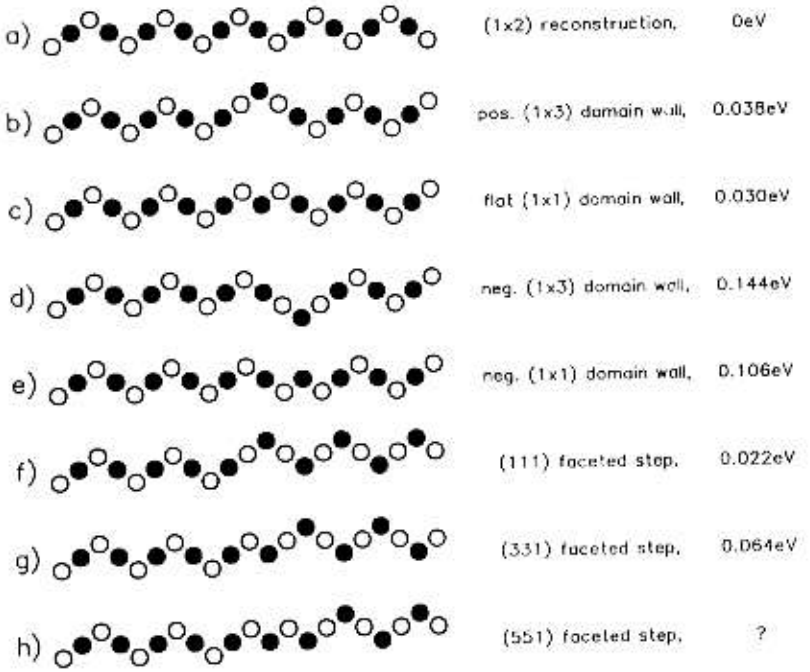

FIGURE 3: Defect structures (side view) of the (1x2) reconstructed fcc (110) surface with creation energies per atom (glue model [28])

In the course of our ion scattering work we used also another approach, i. e. the NICISS variation (Neutral Impact Collision Ion Scattering Spectrometry) [13, 14, 15]. The method is based on the classical shadow cone effect [16]. Fig. 4 shows results of intensity *vs* glancing angle of incidence experiments in comparison with "2 atom-model" calculations [17]. The critical angle which we locate at 0.8 of the intensity is a direct measure of the shadow cone radius at the interatomic distance of the surface chain of atoms in quest on or viceversa [14, 18]. The broadening towards smaller impact angles is a measure for the thermal displacements of the atoms. These displacements can be accurately modelled using the Debye-theory [14]. This is included in the calculations the results of which are the solid lines in Figs. 4. The agreement of experiments and calculation is better than 10^{-4} in most cases (least square deviations). The results of the NICISS experiments are summarized in Fig 5 which shows the intensities related to "perfect" [110] chains, to vacancies in the chains and to larger defects. The appearance of the larger defects at about 650K.

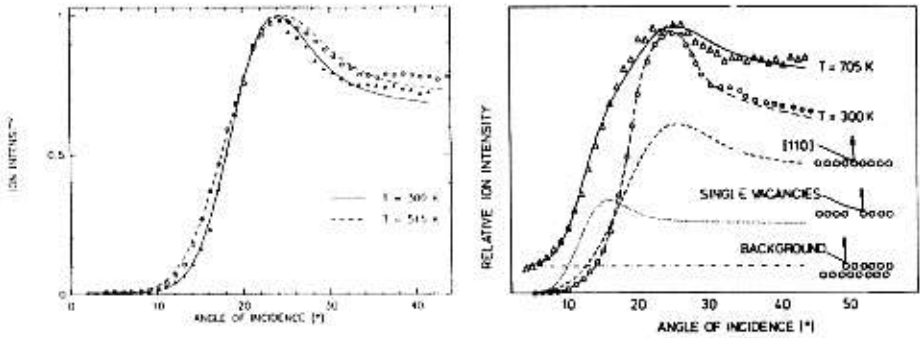

FIGURE 4: Ion scattering results from Au(110) at low temperatures and above the phase transition temperature T_c = 650K. The ion intensities are yields from a NICISS experiment, i. e. double differential spectra with respect to angle and energy making use of the shadow cone effect. Lines are calculated from a two atom model. [17]

(the destruction temperature of the (1x2) structure) [19] is in agreement with the temperature of the roughening transition predicted theoretically [20] and found experimentally [17, 21]. That is, we relate the appearance of the large defects (Fig. 3) with roughening.

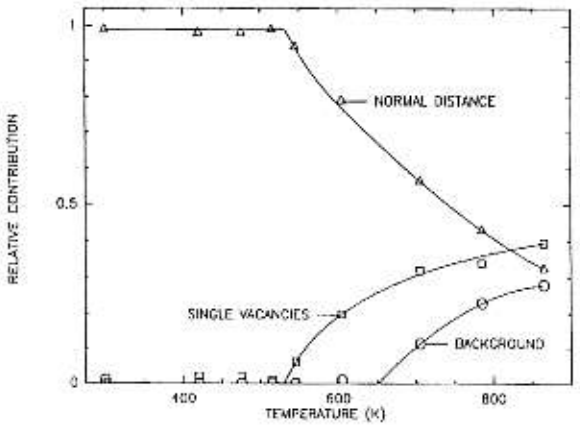

FIGURE 5: Relative contributions of the ion yields in the experiments of Fig. 4 as function of the target temperature. The different contributions are visualized in the inset [17].

The experimental data for the [001] direction show no evidence for other periodicities than (1x2) and a qualitative similar temperature dependence. En passant we mention ISS results for Pt(110) [13, 14, 22] and Ir(110) [23, 24]. In the Pt(110) case (room temperature results only) there is also clear evidence for the missing row structure. The reconstruction is accompanied

by contraction between the first and second layer. The order of the Pt(110) surface is apparently better than that of Au(110) in agreement with STM results [10]. In the Ir(110) case other periodicities are found, i. e. (1x3) mainly mixed with (1x1) and some (1x2). There are also more large defects present at room temperature compared to Au and Pt. In the case of Ir (110) there is also evidence for roughening at about the structure transition temperature of 1050K [25].

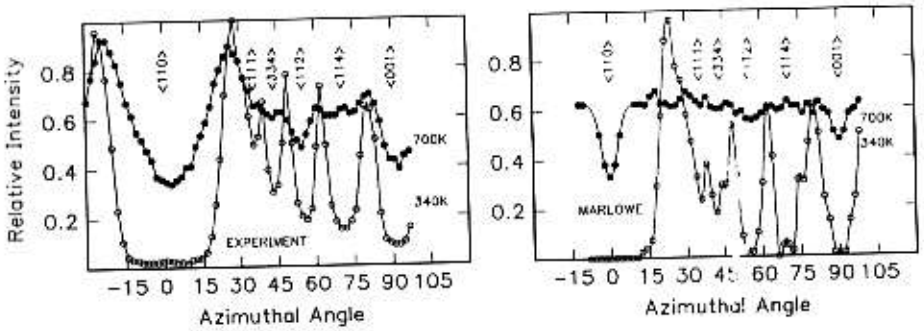

FIGURE 6: Azimuthal dependence of the ion intensity from Au(110)(1x2) at room temperature and above T_c = 650 K, i. e. the phase transition temperature. Each data point is the ion yield of double differential spectrum with respect to angle and energy.

In the last section of this paragraph we will adress the question: what does the Au(110) surface actually look like above the transition temperature of 650K? We have one answer from ion scattering [26, 27] and one from theory [28] the ion scattering results are obtained using the "blocking-effect", i. e. the beam is incident grazingly onto the surface and the ion spectrometer is placed at some large angle of scattering. In the experiment only the azimuthal angle is varied. The result (Fig. 6) is an intensity distribution reflecting the real space periodicity of the crystal, i. e. all low index surface directions cause a minimum in the intensity because all particles are channeled essentially into the specular angle of scattering. Looking at the channeled particles is useful too, i. e. by means of a position sensitive detector [29, 30, 31]. In the blocking pattern, I *vs* φ plot (Fig. 6), "large" channels give wide minima etc. The minimum yield is a measure for the order of the crystal as is the yield of backscattered ions at small angle of incidence in the I *vs* ψ plots (Fig. 4). When the temperature is raised the minima change characteristically but without a "sharp" change at 650K, i. e. the behaviour is rather smooth as in Fig. 5. The increase of the minimum intensity shows, however, a threshold behaviour as the intensity attributed to "background" in Fig. 5. We note that the Au(110) above 650K is certainly not liquid like. A liquid surface causes a flat I *vs* φ curve as shown in the case of surface molten Pb(110) [30]. The comparison with the

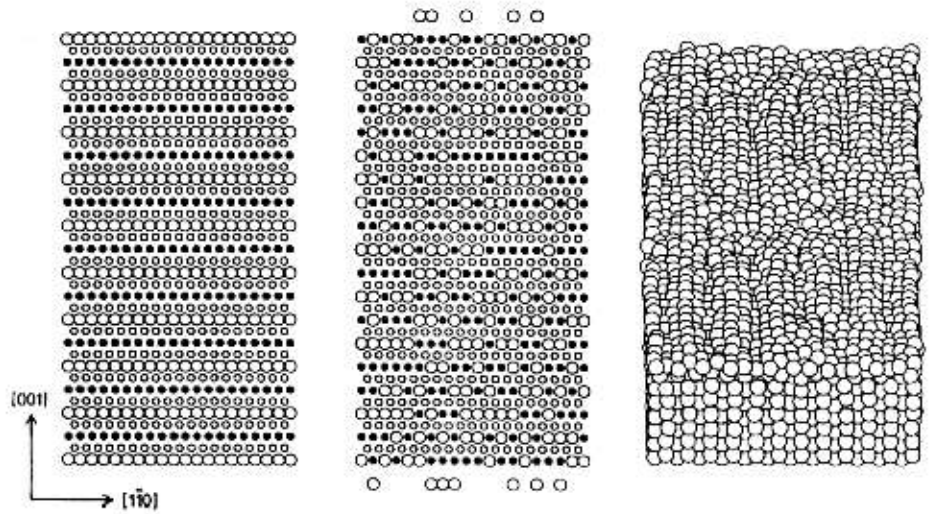

FIGURE 7: Structural models (top view) of the regular (1x2) structure, a "random" model [27], i. e. a randomized $\frac{1}{2}$ monolayer on a regular (1x1) surface, and the disordered structure from glue model calculations [28] (with courtesy of the authors).

MARLOWE [32] results (Fig. 6) is satisfactory at room temperature. The agreement at 700K is bad, probably because the "random" surface model (Fig. 7) used is not the "real" surface structure. We tried other models, e. g. (1x1) with point defects and adatoms, large "anomalous", thermal vibrations etc. with no better results [26]. Qualitatively, Au(110) above 650K is like the rough Pb(110) surface at 420K [33], the detailed structure of which is not known either. A surface as proposed by theory (Fig. 7 right) [28] has not been tested in comparison with our experiments. The theory is based on a "glue potential" calculation. A previous embedded atom (EAM) calculation shows a breakup of the surface chains as in Fig. 7 (middle) but less single atoms or single vacancies [34].

In summary: The pre-STM experiments give a very accurate structure model of Au(110) a good model for the (1x2)⇌(1x1) phase transitions (2D Ising) and some ideas of the disordered surface.

SCANNING TUNNELING MICROSCOPY ON AU(110)

Au(110) was one of the first surfaced probed by STM [35]. The structure was dominantly (1x2) and with practically all the defects expected from the

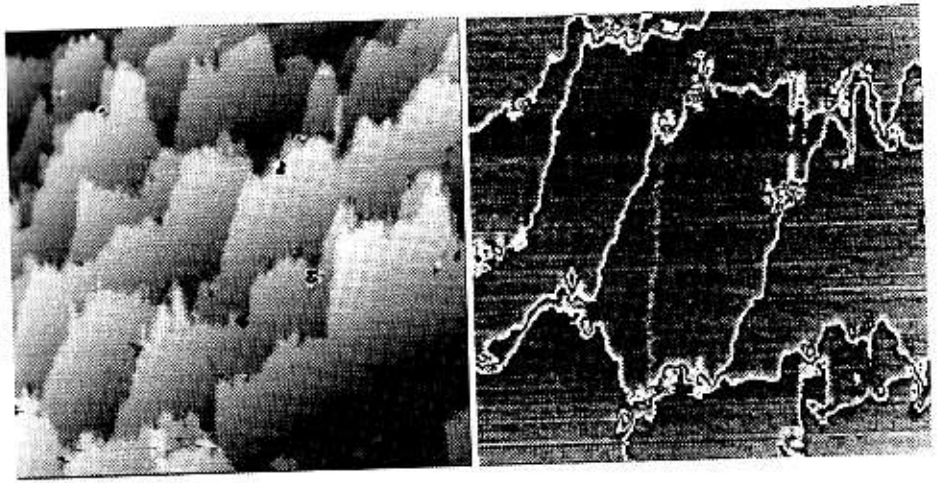

FIGURE 8: left) STM result from a clean, well annealed Au(110)(1x2) surface [12]; (2000 x 2000Å)^2, U_t = 0.5V, I_t = 0.8nA. right) Detail of the structure showing an antiphase domain wall. The top terrace is in the lower right corner. The number of gray scales is equalized to the number of terrace in order to enhance the contrast of the steps and the antiphase domain wall, i. e. the perpendicular line in the middle. (1000 x 1000Å)^2, U_t = 0.5V, I_t = 0.8nA.

previously LEED analysis. Further work on Au(110) [11, 12, 13] led to new results with respect to the step of terrace structure on Au (110). At low but not minimalized impurity levels steps are "pinned" by impurities. Hence rather long (2000Å) terraces are found extending along the [1$\bar{1}$0] direction. The [001] steps are not well defined. The extension of the terraces in the [001] direction is of the order of 50Å in many cases. Usually there are also (1x3) patches on the surfaces. It should be noted that small concentrations of alkali metals on the Au(110) surface cause a (1x2)→(1x3) phase transition [36]. Further cleaning of the surface releases the steps from the pinning situation and the mesoscopic structure has been named "fish scale" structure [10, 11] (Fig. 8). The pattern is enforced by the principle of energy minimization. The free energy/atom in steps is lower for low Miller index steps compared to high Miller index steps. In case of Au(110) the reconstruction makes terraces to have (111) type steps on one side and (331) type steps on the other side (Fig. 9). One example of an antiphase line to compensate for the bordering both sides with (111) steps mainly is shown in Fig. 8 (right). The dominating solution for the problem to have, albeit kinked but (111) type steps mainly, is the "hidden" antiphase by joining three terraces fish scale like. These step structures have not been predicted by any pre-STM work, neither by theory nor by experiment.

So far no STM work has been reported for temperatures above 650K. Up

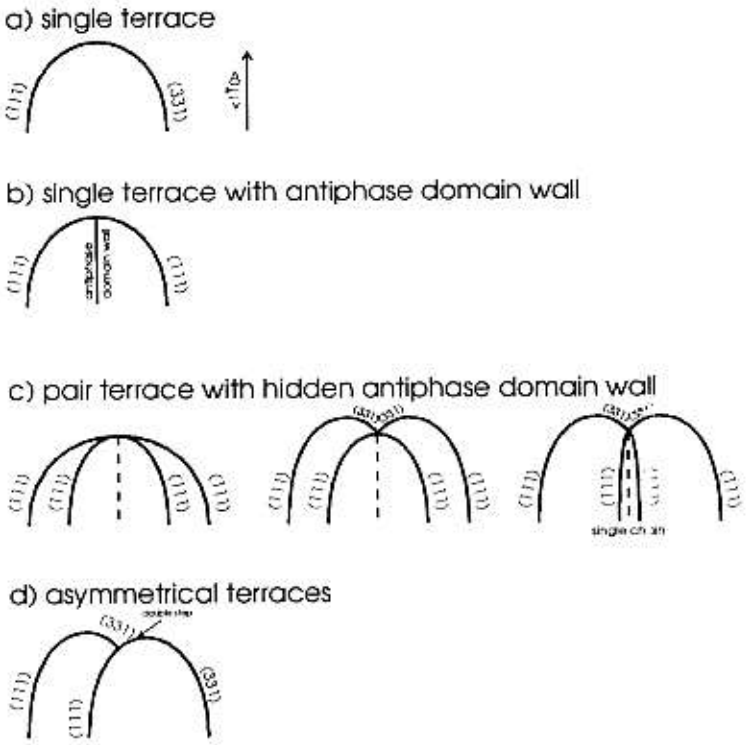

FIGURE 9: Structural models showing the principles possibilities to lower the surface energy by preferentially creating (111) type steps. These steps have the lowest energy compared to e. g. (331) or (001).

to 590K an increasing step mobility is observed manifested by the "frizziness" of the steps due to the fact that the scanning speed becomes smaller than the speed which with the steps are changing their position [37]. Recently we ran STM experiments with "shock cooled", surfaces i. e. the surface was cooled from above 650K with a rate of 50K/min to room temperature. By this means some of the structure of the disordered state is preserved (Fig. 10) [30]. The surface is obviously disordered, but compared to a "random" surface (Fig. 7) the [1$\bar{1}$0] chains are longer than expected compared to the EAM-surface the actual surface is "rougher", i. e. also the second layer is not perfectly ordered. A quantitative analysis of the average distance of the [110] rows shows that there is more (1x3) than (1x2). The preference of the (1x3) distances persists for quite some time in the annealing process. At room temperature it takes

3 days to get the fish scale patterns with a good developed (1x2) structure. The "critical" phase for the shock cooling is probably the interval between 650K and 515K where we found the vacancy formation to start, i. e. the temperature where the surface mobility is high in agreement with the frizziness results [39]. From our STM results we propose that at the (1x1)⇌(1x2) phase transition temperature the [110] chains are not completely randomized. This finding agrees qualitatively with the ion scattering result (Fig. 6) which shows "better" [110] channels than expected from a random model.

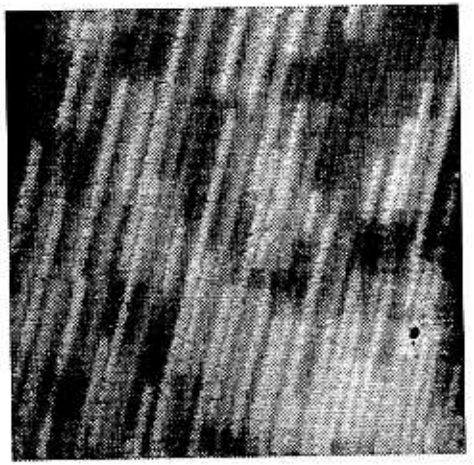

FIGURE 10: STM image from a rapidly cooled Au(110) surface from above 650K to room temperature with a rate of 50K/min. The surface roughness extends over more than two layers. The dominating lattice constant in the [001] direction corresponds on the lighter patches (2nd layer) to a (1x3) reconstruction, on the dark patches (3d layer) to a (1x2) reconstruction. The irregular lengthy rows (light) of the top layer are oriented parallel to [110] (500 x 500 Å^2 $U_t = 0.5V$, $I_t = 0.8nA$).

SUMMARY

The data presented here show clearly that STM is a complementary tool to other surface science techniques including ISS. The strength of STM is the topography information especially about steps and related "defects". Crystallography data are more accurately obtained using pre-STM techniques. High temperature studies may also remain a forbidden realm for STM, since the "capturing" of the tip by the surface atoms under study may be a general effect [40]. A further important difference, as well known as the topography *vs* crystallography arguments [14], is the difference in "chemical" information. It comes naturally e. g. with ISS, but is rather a weak point of STM.

ACKNOWLEDGEMENT

This work is supported by the Deutsche Forschungsgemeinschaft (DFG). T. Rauch, C. Röthig, S. Molitor and J. Bömermann contributed to the STM data represented here.

REFERENCES

[1] Binnig, G., Rohrer, H., Gerber, Ch. and Weibel, E. Phys. Rev. Lett. **49**, 57-61 (1982)

[2] Fedak, D. G. and Gjostein, N. A., Surf. Sci. **8** 77-97 (1967)

[3] Mac Laren, J. M., Pendry, J. B., Rous, P. J., Saln, D. K., Somorjai, G. A., von Hove, M. A. and Vredensky, D. D., Surface Crystallographic Service (Reidel, Dordrecht) 1987

[4] Moritz, W. and Wolf, D., Surf. Sci. **88**, L29-L34 (1979)

[5] Moritz, W. and Wolf, D., Surf. Sci. **88**, L655-L665 (1985)

[6] Overbury, S. H., Heiland, W., Zehner, D. M., Datz S. and Thoe, R. S. Surf. Sci. **109**, 239-262 (1981)

[7] Hemme, H. and Heiland, W., Nucl. Instr. Meth. B **9**, 41-48 (985)

[8] Bonzel, H. P. and Ferrer, S., Surf. Sci. **118**, L263-L268 (1982)

[9] Wolf, D., Habilitationsschrift, Univ. München 1979

[10] Behm, R. J., in: Scanning Tunneling Microscopy and Related Methods, Eds. Behm, R. J., Garcia, N. and Rohrer, H., NATO ASI Series E **184** (Kleuser, Dordrecht) p. 173-209, (1990)
Gritsch, T., Coulman, D., Behm, R. J. and Ertl, G., Surf. Sci. **257**, 297-306 (1991)

[11] Gimzewski, J. K., Berndt, R. and Schittler, R. R., Surf. Sci. **247**, 327-332 (1991) ; Phys. Rev. B**45**, 6844-6857 (1992)
Berndt, R., Gimzewski, J. K. and Schittler, R. R., Ultramicroscopy **42-44**, 528-537 (1992)

[12] Speller, S., Rauch, T. and Heiland, W., Surf. Sci. **324**, 224-232 (1995)

[13] Niehus, H., Surf. Sci. **145**, L 407-418 (1984)

[14] Niehus, H., Heiland, W. and Taglauer, E., Surf. Sci. Rep. **17**, 213-304 (1993)

[15] Aono, M., Hon, Y., Oshima, C., Zaima, S., Otani, S. and Ishizawa, Y., Jpn. J. Appl. Phys. **20**, L829-L835 (1981)

[16] Lindhard, J., Dan, K., Vidensk. Selsk. Mat. Fys.-Medd. **34**, No. 14 (1965)

[17] Riet, E. van de, Derks, H. and Heiland, W., Surf. Sci. **234**, 53-62 (1990)

[18] Hetterich, W., Derks, H. and Heiland, W., Appl. Phys. Lett. **52**, 371-372 (1988)

[19] Campuzzano, J. C., Foster, M. S., Jennings, G., Willis, R. F. and Unertl, W. N., Phys. Rev. Lett. **54**, 2684-2687 (1985)

[20] Villain, J., and Vilfan, I., Surf. Sci. **199**, 165-173 (1988)

[21] Sprösser, J., Salanon, B., and Lapujoulade, J., Europhys. Lett. **16**, 283-287 (1991)

[22] Masson, F. and Rabalais, J. W., Surf Sci **253**, 245-257 (1991)

[23] Hetterich, W. and Heiland, W. Surf. Sci. **210** 129-137 (1989)

[24] Bu, H., Shi, M., Mason, F. and Rabalais, J. W., Surf. Sci. Lett. **290**, L140-L146 (1990)

[25] Hetterich, W. Höfner, C. and Heiland, W. Surf. Sci. **151/152** 731-736 (1991)

[26] Derks, H., Möller, J. and Heiland, W., Springer Series in Surf. Sci. **11**, 469-561 (1988)

[27] Derks, H., Hetterich, W., Riet, E. van de, Niehus, H. and Heiland, W., Nucl. Instr. Meth. **B48** 315-318 (1990)

[28] Bernasconi, M. and Tosatti, E., Surf. Sci. Rep. **17**, 363-422 (1993)

[29] Niehof, A. and Heiland, W., Nucl. Instr. Meth. **B48**, 306-310 (1990)

[30] Speller, S., Schleberger, M., Niehof, A. and Heiland, W., Phys. Rev. Lett. **68** 3452-3455 (1992)

[31] Schleberger, M., Speller, S., Höfner, C. and Heiland, W., Nucl. Instr. Meth. **B90**, 274-276 (1994)

[32] Robinson, M. T. and Torrens, I. M., Phys. Rev. **9**, 5008-5024 (1974)

[33] Speller, S., Schleberger, M., Franke, H., Müller, C and Heiland W., Mod. Phys. Lett. **B8** , 491-503, (1994)

[34] Daw, M. S. and Foiles, S. M., Springer Series in Surf. Sci. **11**, 125-131 (1988)

[35] Binnig, G., Rohrer, H., Gerber, Ch. and Weibel, W., Surf. Sci **131**, L379-L384 (1985)

[36] Häberle, P., Fenter, P. and Gustafsson, T., Phys. Rev. **B39**, 5810 (1989)

[37] Kuipers, L., Hoogeman, M. S. and Frenken, J. W. M., Phys. Rev. Lett. **71**, 3517-3520 (1993)

[38] Speller, S., Molitor, S., Röthig, C., Bömermann, J. and Heiland, W. Surf. Sci. **312**, L748-L752 (1994)

[39] Kuipers, L., Thesis Amsterdam 1994

[40] Kuipers, L. and Frenken, J. W. M., Phys. Rev. Lett. **70**, 3907-3910 (1993)